

Abundance analysis of 5 early-type stars in the young open cluster IC 2391 [★]

Ch. Stütz^{1,2}, S. Bagnulo², E. Jehin², C. Ledoux², R. Cabanac³, C. Melo² and J.V. Smoker^{2,4}

¹ Institute of Astronomy (IfA), University of Vienna, Türkenschanzstrasse 17, A-1180 Vienna, Austria

² European Southern Observatory, Casilla 19001, Santiago 19, Chile

³ Canada-France-Hawaii Telescope Corporation, 65-1238 Mamalahoa Hwy. Kamuela, Hawaii 96743, USA

⁴ Astrophysics & Planetary Science Research Division, Department of Physics and Astronomy, The Queen's University of Belfast, University Road, Belfast, BT7 1NN, U.K.

Received; accepted

ABSTRACT

Aims. It is unclear whether chemically peculiar stars of the upper main sequence represent a class completely distinct from normal A-type stars, or whether there exists a continuous transition from the normal to the most peculiar late F- to early B-type stars. A systematic abundance analysis of open cluster early-type stars would help to relate the observed differences of the chemical abundances of the photospheres to other stellar characteristics, without being concerned by possible different original chemical composition. Furthermore, if a continuous transition region from the very peculiar to the so called normal A–F stars exists, it should be possible to detect objects with mild peculiarities.

Methods. As a first step of a larger project, an abundance analysis of 5 F–A type stars in the young cluster IC 2391 was performed using high resolution spectra obtained with the UVES instrument of the ESO VLT.

Results. Our targets seem to follow a general abundance pattern: close to solar abundance of the light elements and iron peak elements, heavy elements are slightly overabundant with respect to the sun, similar to what was found in previous studies of normal field A-type stars of the galactic plane. We detected a weakly chemically peculiar star, HD 74044. Its element pattern contains characteristics of CP1 as well as CP2 stars, enhanced abundances of iron peak elements and also higher abundances of Sc, Y, Ba and Ce. We did not detect a magnetic field in this star (detection limit was 2 kG). We also studied the star SHJM 2, proposed as a pre-main sequence object in previous works. Using spectroscopy we found a high surface gravity, which suggests that the star is very close to the ZAMS.

Key words. Open clusters and associations: individual: IC2391 – Stars: abundances – Stars: evolution – Stars: chemically peculiar – Stars: pre-main sequence

1. Introduction

The atmospheres of main sequence A-type stars should be relatively simple to understand and to model. Convection is apparently absent, stellar winds are very weak, and little or no photospheric microturbulence is generally present. Yet, in this group of stars, a large variety of peculiarities are observed. Among A- and B-type stars, about 10% are chemically peculiar, i.e., the analysis of their spectra reveal overabundances (e.g., of iron-peak and/or rare-earths elements) and/or underabundances (e.g., of He, Ca, and Sc), compared to the composition of the solar photosphere. Many of these chemically peculiar (CP) stars exhibit large scale magnetic fields with a typical strength of a few hundreds up to a few tens of thousands of Gauss. Furthermore, many of the CP stars reveal very in-

homogeneous atmospheric distributions of numerous elements. Another characteristic of CP stars is that, compared to the normal A and B-type stars, most have long rotation periods – typically several days, but up to a few decades for some magnetic CP stars. For a more detailed introduction to the variety of phenomena observed in A and B-type stars see, e.g., Preston (1974), Wolff (1983).

An important question to address is whether the CP stars represent a group that is well separated from “normal” A and B-type stars, or whether CP stars are the extreme cases of a group of stars spanning all grades of peculiarity. If a continuous transition from the very peculiar to the so called normal A–F stars exists, it should be possible to detect objects with mild peculiarities.

There are several reasons why these stars are so difficult to identify. Rotation velocities of normal A-type stars are in most cases too high ($\langle v \sin i \rangle \sim 150 \text{ km s}^{-1}$) to allow precise abundance determination. Pronounced chemical peculiar-

Send offprint requests to: Ch. Stütz

[★] Based on observations made with ESO Telescopes at the Paranal Observatory under programme ID 266.D-5655

ity is mostly found in slow rotators ($\langle v \sin i \rangle \sim 40 \text{ km s}^{-1}$), whereas studying a transition from CP to normal stars also implies analysing objects with higher projected rotation velocities. Thus it is not clear whether this anticorrelation of $v \sin i$ and peculiarity is a physical one, or if it is due to a selection effect. In other words, is rotation preventing chemical peculiarity or is it hiding chemical peculiarity? Hill and Landstreet (1993) explicitly showed for narrow lined A stars ($v \sin i \lesssim 25 \text{ km s}^{-1}$) of the galactic plane that the variations in the individual elemental abundances can be quite large (± 0.4 dex). The same is reflected in the work of Adelman and collaborators (e.g. Kocer et al. 2003, Pintado & Adelman 2003).

The proper way to address the questions above is to perform a detailed abundance analysis of early-type stars of different ages and rotational velocities. Members of open clusters are of special interest because one can safely assume that members of the same cluster are more or less of the same age and chemical composition. They should differ from each other only by their initial mass. Furthermore, the cluster age can be determined with much more accuracy than the age of individual stars in the field. We thus carried out a detailed study of 5 main sequence stars of spectral type B – F belonging to the young open cluster IC 2391. For our investigations we used spectra obtained with UVES, the high resolution spectrograph of the ESO VLT. As the stars of IC 2391 we analysed are roughly the same age and were formed from similar initial chemical composition, we expect that if significant deviations from the abundance pattern typical for IC 2391 are found, they will be nearly independent of these two stellar properties. Thus the probability that weak chemical peculiarity dates back to the birth of the star is higher than for stars located in the galactic field. Since the cluster is very young (~ 36 Mys, Lyngå 1987), main sequence (MS) evolutionary effects are small. One star of our sample, SHMJ 2, may have not reached the MS yet.

2. Observations and data reduction

2.1. Observations

IC 2391 was observed from 7 to 12 February 2001 with the UVES instrument of the ESO VLT Unit 2 Kueyen within the framework of the UVES Paranal Observatory Project (Bagnulo et al. 2003). Target selection was performed mainly with the WEBDA open cluster database ([HTTP://WWW.UNIVIE.AC.AT/WEBDA/](http://www.univie.ac.at/webda/)) developed by J-C. Mermilliod at the Institute for Astronomy of the University of Lausanne and maintained by E. Paunzen at the University of Vienna. Some additional pre-main sequence stars were selected using the work by Stauffer et al. (1989). Spectra for about 50 candidate cluster members were obtained using the settings DIC1 (346+580) and DIC2 (437+860) (see UVES user manual VLT-MAN-ESO-13200-1825) with a $0.5''$ slit width. The resulting spectra cover almost the entire spectral range from 305 nm to 1040 nm with a spectral resolution of about 80 000. The raw data are available at the ESO archive under programme ID 266.D-5655.

2.2. Target selection

In total, 50 stars of IC 2391 were observed. For 8 early-type stars among them, the rotational velocity is low enough and the quality of the spectral data sufficient for our purposes of detailed abundance analysis. These stars are listed in Table 1.

Information about membership was extracted from Robichon et al. (1999), Levato et al. (1988), Perry & Hill (1969), and Stauffer et al. (1989). Membership was cross-checked using Hipparcos parallaxes, the most recent $E(b - y)$ data found in the SIMBAD database and new radial velocity measurements of UVES POP stars by Noterdaeme et al. (in preparation). For two objects of Table 1, membership remains questionable. HD 75029 is not stated as a member in Perry & Hill (1969), however, its astrometric parameters agree well with the cluster mean. On the other hand HD 73778, according to Levato et al. (1988), very likely is not a member of IC 2391. The Si star HD 74535 was investigated by Lüftinger et al. (in prep.) parallel to our study. We analysed HD 73722, HD 74044,

Table 1. Candidate target stars for abundance analysis. Rotation velocities from Noterdaeme et al. (in preparation). M? denotes questionable membership, $v \sin i$ in km s^{-1} . The Δa index that is sensitive to CP2 type peculiarity is taken from Maitzen & Catalano (1986). A * indicates stars that were selected for the abundance analysis.

star	sp.type	m_v	$v \sin i$	notes
HD 73722	F5 V	8.92	6.8	*
HD 73778	F0 V	8.76	40	M?
HD 74044	A3	8.48	32	$\Delta a = 1$, Am? *
HD 74275	A0 V	7.27	62	*
HD 74535	B8	5.55	37	$\Delta a = 26$, Si
HD 75029	A2/3	9.45	24	$\Delta a = -7$, M? *
CPD -52 1568	F5 V	9.62	19	
SHJM 2	F9	10.3	10	PMS? *

HD 74275, HD 75029 and SHJM 2. This target selection is the result of a compromise between keeping the spread of spectral types large and the projected rotation velocities low.

2.3. Data reduction

Data have been reduced by the UVES POP team using an automatic procedure based on the MIDAS UVES pipeline (Ballester et al. 2000). Science frames were bias-subtracted and divided by the extracted flat-field, except for the 860 setting, where the 2D (pixel-to-pixel) flat-fielding was used in order to better correct for fringing. Because of the high flux of the spectra the *average extraction* method was used instead of the *optimal extraction* method that is recommended for spectra characterised by a signal to noise ratio (SNR) $\lesssim 100$. Further details about the reduction procedure can be found in Bagnulo et al. (2003). All reduced spectra can be obtained with the UVES POP web interface at [HTTP://WWW.ESO.ORG/UVESPOP/](http://www.eso.org/uvesspop/).

Taking advantage of the quality control parameters produced by the UVES pipeline, we performed a check of the instrument stability and actual performance. The accuracy of

the wavelength calibration was found to be of the order of 300 ms^{-1} only because the Th-Ar reference frames were taken the following morning and not before and after each observation (the temperature difference between science exposures and calibrations was typically 1 K). For this work we used the following wavelength intervals: 3730–4990 Å (characterised by a mean resolution $\langle R \rangle = 76\,000$ and a SNR of 100–150); 4760–5770 Å ($\langle R \rangle = 82\,000$ and SNR = 210–150); 5840–6840 Å ($\langle R \rangle = 73\,000$ and SNR = 170–130). We found a maximum variation of 3.7 % for these mean resolutions.

2.4. Continuum normalisation

The targets selected for the abundance analysis include objects with rotation velocities up to $\approx 60 \text{ km s}^{-1}$. For such fast rotating stars, the determination of the elemental abundances depends critically on the accuracy of the continuum normalisation. To be sure to perform accurate continuum fitting, we performed some tests using the spectra of HD 74169, a slow rotating cluster member Ap star that will be analysed in detail in a forthcoming paper by Lüftinger et al. We normalised the star’s high SNR (≈ 300) spectra in two independent ways: Using the merged output of the UVES pipeline, and using the intermediate “2D unmerged” spectra, i.e., the spectra corresponding to the individual echelle orders (also available through the UVES POP web interface). The fully merged spectra are affected by some artefacts mainly due to an imperfect merging of the echelle orders (for details see Bagnulo et al. 2003 and references therein), hence better results are expected to be obtained by normalisation of the unmerged spectra. However, an optimum normalisation could be obtained by dividing the merged spectra into sub-spectra of a maximum length of 100 Å, and by treating these individually. This way we obtained an agreement to better than 1 % over the whole spectral range for the two different techniques. The maximum size of the differences in the normalised spectra obtained with the two methods does not generally occur at the wavelengths of the extremes of the echelle orders. This suggests that the order merging performed by the UVES pipeline is sufficiently accurate and does not lead to major artefacts in the abundance analysis.

Our comparison showed that we could not clearly define the continuum for the hydrogen lines (which are in general broader than 100 Å) and thus we did not use them to determine fundamental atmospheric parameters.

To identify telluric lines we used the star HD 74196 as reference. The spectrum of this cluster member does not contain many lines (spectral type B7V) which are heavily broadened due to the high rotational velocity of $v \sin i = 300 \text{ km s}^{-1}$.

3. Abundance analysis

The starting values for the fundamental parameters of the atmosphere of the selected stars were estimated via Strömgren photometry (Johnson *UBV* photometry in the case of SHJM 2) and evolutionary tracks for the cluster interpolated from Schaller et al. (2004). The uncertainties of these estimates are quite large (typically 200 K in T_{eff} and 0.25 in $\log g$), thus we tried to improve the fundamental parameters by spectroscopic means.

T_{eff} estimates were improved via elimination of an abundance– χ_{excit} correlation (see Fig. 1). $\log g$ estimates were improved by making sure that there is no systematic difference in abundances between different ionisation stages of chemical elements (called in the following “ionisation equation condition”). The presence of a magnetic field was checked looking at the correlation of abundances with Landé factors, and by searching for magnetically split lines. Together with the mean metallicity

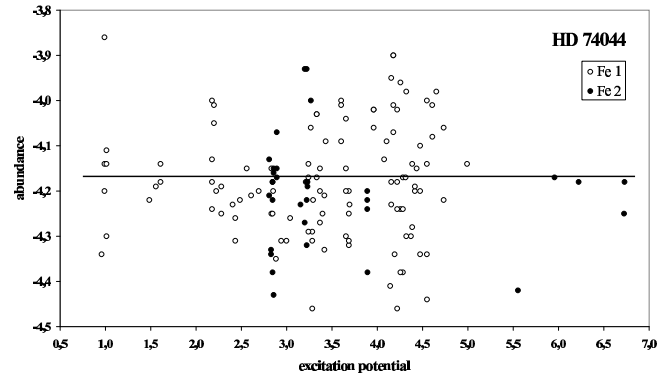


Fig. 1. Excitation potential vs. abundance for the final values of T_{eff} and $\log g$ of HD 74044. Open circles – FeI, filled circles – FeII. A least squares linear regression yields: $\text{abn} = -0.0002\chi_{\text{excit}} - 4.18$.

of the cluster ($[\text{Fe}/\text{H}] = -0.03$, Randich et al. 2001), these parameters defined the first atmosphere calculated with LLmodels (Shuliak et al. 2004) in ODF mode (ODF: estimating line absorption via a pre calculated opacity distribution function). Using this model we calculated the emerging flux at the center of lines extracted from the VALD database (Piskunov et al. 1995, Kupka et al. 1999, Ryabchikova et al. 1999) and pre-selected only those that make an important contribution to the opacity ($\kappa_{\nu L}/\kappa_{\nu C} \geq 1\%$, $\kappa_{\nu L}$ and $\kappa_{\nu C}$ are the line and continuum absorption coefficient).

We determined the initial microturbulence and element abundance pattern from equivalent widths of unblended lines using the *widthV* software written by V. Tsymbal. Assuming that for our set of spectral lines non-LTE and stratification effects are negligible, there should be no correlation between abundances determined from the equivalent widths and the widths themselves or the excitation energy, and the ionisation equation condition should be fulfilled. Eliminating the above correlations for the elements where we found the most unblended or marginally blended lines in the spectra (typically Fe, Cr, Ti, Ni, Ca) resulted not only in a fairly good determination of microturbulence and first abundances, but also in an improvement of effective temperature and surface gravity. For HD 74275 we had to perform this step via synthetic line fitting, since this star rotates with $v \sin i = 60.5 \text{ km s}^{-1}$ and shows only a few unblended lines. For synthetic line fitting all our models were calculated with LLmodels in the line-by-line modus (Shuliak 2004). This means that the individual abundance pattern is included in our atmospheric models as well. The hydrogen lines were treated using VCS theory (Vidal, Cooper and Smith 1973). Convection was mod-

elled according to the formalism of Canuto and Mazzitelli (1991). For atmospheric modelling as well as for the line synthesis with Synth3 (Piskunov 1992 and Valenti et al. 1998) we extracted the atomic lines from the VALD line database. To analyse the spectra, in the sense of deriving noise, deviations between observed and synthesized spectra, measuring equivalent widths, etc., we developed the 'Little Spectrum Analyser' (Lispan). The graphical interface for the codes which also controls the automatic line core fitting is called ATC. The set of atmospheric modelling and analysis software used for this investigation can be reviewed on the web at [HTTP://AMS.ASTRO.UNIVIE.AC.AT/COMPUTER/CHRSOFT/CHRSOFT.HTML](http://ams.astro.univie.ac.at/computer/chrssoft/chrssoft.html) Once we had fixed $v \sin i$ and v_{mic} (see Table 2) by synthetic line fitting of the unblended lines, we determined the elemental abundances in an iterative process:

- Automatic line core fitting with ATC, Synth3 and Lispan. This is faster than fitting the whole line, but one has to be sure of $v \sin i$, v_{mic} and if present, the magnetic field. The only free parameters here are the abundances.
- Check for peculiarities and magnetic fields.
- Fine tuning of fundamental parameters (T_{eff} , $\log g$, v_{mic} , $v \sin i$). Check the conditions mentioned above and whether they hold when peculiarities have been found.
- Edit line selection if blends have been overlooked, certain lines show non-LTE effects, the quality of line parameters are uncertain, etc.

This procedure resulted in fundamental atmospheric parameters with internal errors lower than 150 K in T_{eff} , 0.20 dex in $\log g$, 0.20 kms^{-1} in v_{mic} , 0.3 kms^{-1} in $v \sin i$ and accurate element abundances (0.1 – 0.3 dex in general) for all the program stars except HD 75029 which very likely is a spectroscopic binary. For more detailed discussions on internal and absolute errors in modern abundance analyses see Andrievsky et al. (2002) or Hill & Landstreet (1993).

4. Results

The atmospheric parameters of our stars were checked by fits of the H lines. Atomic lines blended by the wings of H Balmer lines were not used for abundance analysis because we could not precisely determine the continuum. In some cases the number of lines suitable for deriving abundances of a certain element was very small. For four stars these lines are listed in Table 5. For the star HD 74044 the complete list of lines used for the abundance analysis is presented in Table 4. We found no indications for mean magnetic surface fields larger than 1 kG in HD 73722, HD 75029 and SHJM 2, or larger than 2 kG in HD 74044 and HD 74275. We did not find any published high quality abundance analyses of stars of IC 2391 for a comparison with our work. In the following we will present the results for the 5 stars we have analysed.

HD 74044: For HD 74044 we determined a projected rotation velocity of 33.7 kms^{-1} . Fundamental atmospheric parameters were derived from Fe, Ca, Cr, Mg, Ni and Ti. We could determine relatively precise abundances for 10 elements and abundance estimates for C, Ce, Cu, Mn, O, Y and Zn (see Table 3).

Comparing the abundance pattern of HD 74044 to the other stars we see indications for a mild chemical peculiarity, which is supported by the higher abundances of Sc, Y, Ba and Ce (Fig. 2). The element pattern of HD 74044 contains character-

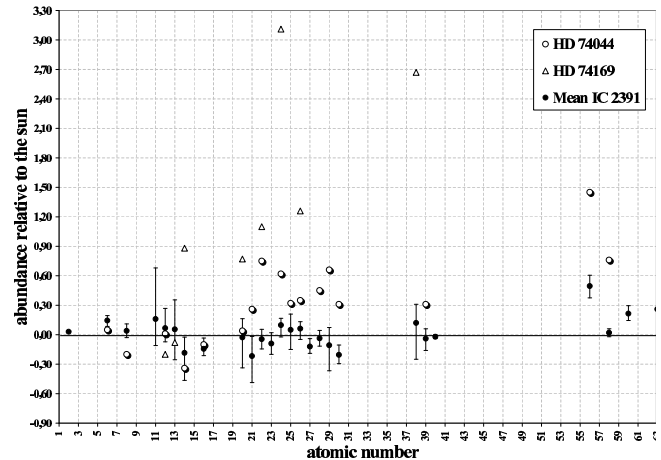


Fig. 2. Comparison of the abundances in HD 74044 (open circles) with those of the CP star HD 74169 (open triangles, Lüftinger, in prep.) and to the mean of the other members of IC 2391 (filled circles). Abundances are in units of $[N_{\text{El}}/N_{\text{tot}}] - [N_{\text{El}}/N_{\text{tot}}]_{\odot}$ (solar abundances according to Grevesse and Sauval 1998). Error bars indicate maximum deviations from the mean.

istics of CP1 stars (enhanced iron peak elements) as well as CP2 stars (enhanced Sc, and heavy elements). A similar pattern but much more pronounced can be seen in the cluster star HD 74169 known to be of type CP2 (Lüftinger et al, in prep.). Due to the rotation velocity of 33.7 kms^{-1} our detection limit for a mean surface magnetic field is about 2 kG. Polarimetric observations will be necessary to check for the presence a magnetic field.

HD 73722: This slowly rotating star ($v \sin i = 6.7 \text{ kms}^{-1}$) is listed in the catalogue of eclipsing and spectroscopic binary stars by Popova & Kraicheva (1984). But after carefully scanning our spectra we found no hints of line patterns that could originate from a stellar companion or a close background star. Temperature, surface gravity and microturbulence (Table 2) were confirmed with lines from Fe, Cr, Ti, Ni, Ca, Si and Mn. TiII and TiIII deviated noticeably from the ionisation equilibrium condition. Their abundances are -7.08 and -7.16 respectively. Typical for this analysis was $|[N_{\text{El}}/N_{\text{tot}}]_{\text{I}} - [N_{\text{El}}/N_{\text{tot}}]_{\text{II}}| < 0.05$ for different ionisation stages of the same element. The abundance of Sr is uncertain because both lines we analysed (SrII 4161.792 Å and SrI 4607.327 Å) are blended. The result for oxygen should be considered as an upper limit.

HD 74275: With $v \sin i = 60.5 \text{ kms}^{-1}$, this is the fastest rotating star we have analysed. It is also the hottest one. Thus only few lines could be used and the quality of our Ca, O, Si and Na abundances is not as good as our internal error estimates

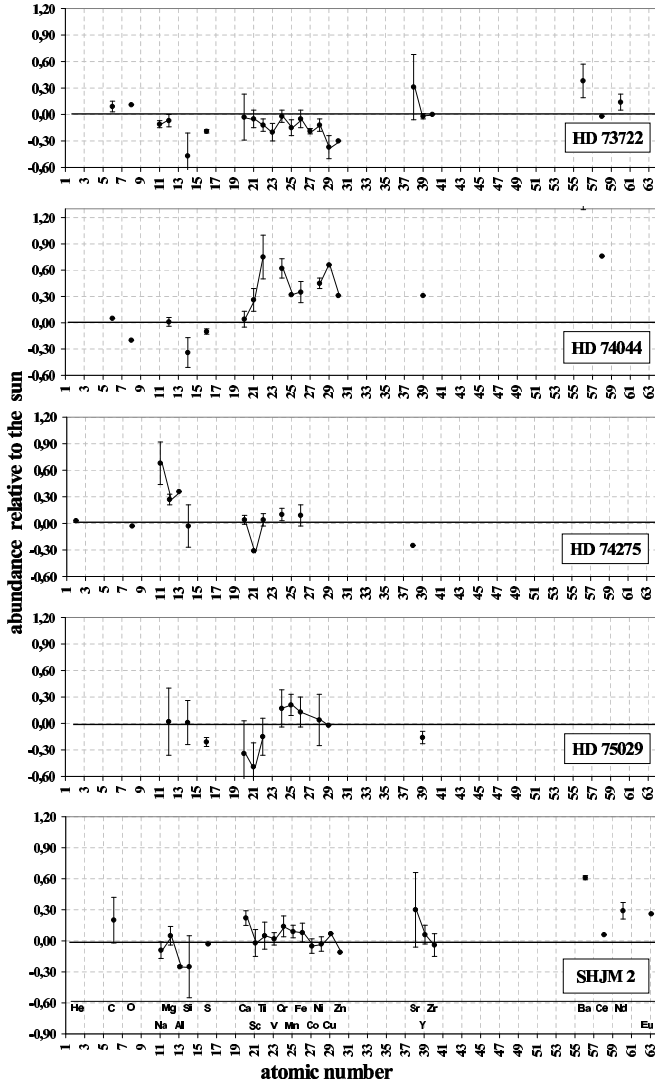


Fig. 3. Elemental abundances relative to the sun. Solar values according to Grevesse and Sauval (1998). Data points of elements with consecutive atomic numbers are connected with lines. Errors as in Table 3.

may suggest. The atmospheric parameters were refined from Fe, Cr, Ti and Mg. In 5 lines (Na I 5889.951, Na I 5895.924, Si II 6347.109, Si II 6371.371 and He I 5875.615) we corrected for atmospheric features (see sect.2.4). The remarkable overabundance of Na (≈ 0.7 dex) is probably a non-LTE effect we could not account for. Takeda (2003) and Asplund (2005) both suggest non-LTE abundance corrections of up to -0.5 dex for these two lines. The abundance of helium, determined from 1 line (He I 5875.615 Å), is more or less solar.

HD 75029: Although the membership of this star may be questionable, we included it in our analysis, since it was the only slowly rotating star ($v \sin i = 22 \text{ km s}^{-1}$) with spectral type between A0 and F5 and no known peculiarities. *A posteriori* we found that its abundances fit quite well in the overall pattern we see for IC 2391. The star very likely has a faint fast rotating spectroscopic companion, also noticed by Popova &

Kraicheva (1984). We could not directly separate the spectrum of the companion, but we found our continuum to be systematically too low for regions around deeper lines. Strong contamination due to twilight can be ruled out as the cause because we do not see this behaviour in the spectra of HD 74275 which has been observed at a time even closer to dawn. Unfortunately no details about the possible companion are known so far, hence our results for HD 75029 are not as accurate as they should be.

SHJM2: Using the UVES observations we could analyse in detail the spectrum of a very slowly rotating ($v \sin i = 10.6 \text{ km s}^{-1}$) possible PMS star. Stauffer et al. (1989 and 1997) suggested that SHJM 2 has not yet reached the ZAMS. The surface gravity we determined by spectroscopic means ($\log g = 4.40$) is surprisingly high if we consider the star to be a PMS object. Evolutionary tracks for cluster stars give the same value for cluster members with this effective temperature situated on the ZAMS. Therefore SHJM 2 is probably at the very end of its pre main sequence phase or has already reached the ZAMS. Since SHJM 2 is already in the final stage of its PMS phase and very close to the main sequence, we applied the techniques developed for main sequence stars for an abundance analysis. Examining the iron lines Fe I 6149.258 and Fe I 6336.8243 we could detect no magnetic field. The star generally reflects the pattern of the other cluster members (except HD 74044 of course).

5. Discussion and conclusions

We have carried out a detailed analysis of the atmospheres of 5 A–F stars in the cluster IC 2391 and have obtained reasonably accurate fundamental parameters and element abundances accurate within 0.1 – 0.3 dex. Specific element patterns were included in our atmospheric models and the presence of magnetic fields and the possibility of stratification were checked too (when $v \sin i \leq 25 \text{ km s}^{-1}$).

Understanding HD 74044 contributes to our knowledge of the A star phenomenon. This star shows a mild peculiarity of the type CP1 and CP2: Sc, Ti, Cr, Mn, Fe, Ni, Cu, Zn, Y and Ce are enhanced by 0.3 – 0.8 dex relative to the mean of the other cluster members, and even more so Ba. Nevertheless we neither can confidently assign HD 74044 to the group of CP2 nor CP1 stars. We situate this object in the continuous transition region from the very peculiar to the normal A–F stars. We did not detect a magnetic surface field, but our detection limit is rather high (2 kG). Therefore follow-up polarimetric observations are necessary to clarify its status.

The abundance star to star scatter of the other cluster stars is, as expected, small (0.1 – 0.3 dex) compared to what was found for stars in the galactic plane (0.3 – 0.5 dex) by Hill & Landstreet (1993) and Hill (1995) for 6 and 9 objects respectively. A comparison of a cluster abundance pattern derived in this work for 26 elements to the abundances of early A stars in the galactic plane is shown in Figure 4. Note that not only the star to star variations of element abundances are larger in the galactic plane, but they also seem to increase for faster rotating stars. The latter may not be an intrinsic effect of rota-

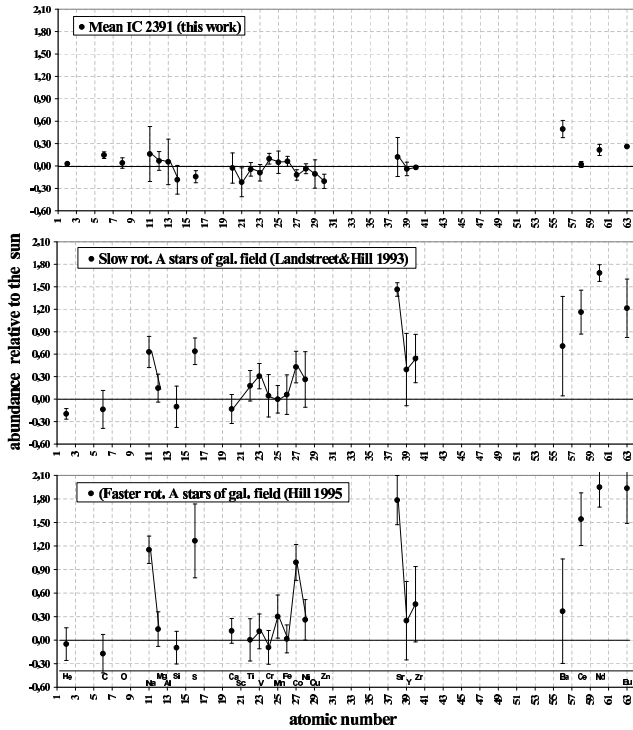


Fig. 4. Mean abundance pattern of IC 2391 (HD 74044 excluded) derived in this work compared to the abundance pattern found for field stars by Hill & Landstreet (1993) and Hill (1995). Elemental abundances are relative to the sun with solar values according to Grevesse and Sauval (1998). Data points of elements with consecutive atomic numbers are connected with lines. Error bars are variances of the mean abundances.

tion, but due to the fact that detailed abundance studies become rather difficult for faster rotating stars. For the needed accuracy our technique is limited to a $v \sin i \leq 60.5 \text{ km s}^{-1}$, measured for HD 74275.

Our sample includes the star SHJM 2, probably a PMS star already close to the ZAMS considering the findings of Stauffer et al. (1989) and the star's high surface gravity. Assuming that its atmosphere can be modelled applying the same physics and approximations as for MS A–F stars, we performed a detailed abundance analysis in the optical range for this star. Its abundances reflect the general abundance pattern of IC 2391.

Acknowledgements. We like to thank Theresa Lüftinger for insight in her analysis of HD 74169 and Pasquier Noterdaeme for his most recent $v \sin i$ data for this cluster. We also thank Martin Stifft for his helpful suggestions on presentation of the results. Ch. Stütz acknowledges ESO DGDF for a three month studentship at ESO Santiago/Vitacura and the FWF (project P17890).

References

Andrievsky, S.M., Chernyshova, I.V., Paunzen, E., et al., 2002, *A&A*, 396, 64
 Asplund, M., Grevesse, N., & Sauval, A.J., 2004, *The solar chemical composition, Cosmic Abundances as Records of Stellar Evolution and Nucleosynthesis ASP Conference Series, Vol. 30*, F.N. Bash and T.G. Barnes (eds.)

Asplund, M. 2005, *ARA&A*, 43, 481
 Bagnulo, S., Jehin, E., Ledoux, C., et al. 2003, *ESO Messenger*, 114, p. 10
 Ballester, P., Modigliani, A., Boitquin, O., et al. 2000, *ESO Messenger* 101, p. 31
 Canuto, V.M., & Mazzitelli, I. 1991, *ApJ*, 370, 295–311
 Grevesse, N., & Sauval, A.J. 1998, *SSR*, vol. 85, 161–174
 Hill, G.M., & Landstreet, J.D. 1993, *A&A*, 276, 142
 Hill, G.M. 1995, *A&A*, 294, 536
 Levato, H., Garcia, B., Lustó, C., & Morrell, N. 1988, *Ap&SS*, 146, 361
 Kocer, D., Adelman, S.J., Caliskan, H., Gulliver, A.F., & Gokmen Tektunali, H. 2003, *A&A*, 406, 975
 Kupka, F., Piskunov, N.E., Ryabchikova, T.A., Stempels, H. C., & Weiss, W.W. 1999, *A&AS*, 138, 119
 Landstreet, J.D. 2004, in: *The A-Star Puzzle*, Zverko, J., Ziznovsky, J., Adelman, S.J., & Weiss, W.W. (eds.) *IAUS 224*, 423
 Levato, H., Garcia, B., Lustó, C., & Morrell, N. 1988, *Ap&SS*, 146, 361
 Lyngå, G., 1987, *Catalog of open cluster data (5th edition)*
 Maitzen, H.M., & Catalano, F.A. 1986, *A&AS* 66, 37
 Perry, C.L., & Hill, G. 1969, *AJ*, 74, 899
 Pintado, O.I., & Adelman, S.J., 2003, *A&A*, 406, 987
 Piskunov, N., 1992, *Stellar Magnetism - Proceedings of the international meeting on the problem Physics and Evolution of Stars*, Yu. V. Glagolevskij and I. I. Romanyuk (eds.), St. Petersburg, p. 92
 Piskunov, N.E., Kupka, F., Ryabchikova, T.A., Weiss, W.W., & Jeffery, C.S. 1995, *A&AS*, 112, 525
 Popova, M., & Kraicheva, Z. 1984, *Astrofizik. Issledovanija*, 18, 64–88
 Preston, G.W. 1974, *ARA&A*, 12, 257
 Randich, S., Pallavicini, R., Meola, G., Stauffer, J.R., & Balachandran, S.C. 2001, *A&A*, 372, 862
 Robichon, N N., Arenou, F., Mermilliod, J.-C., and Turon, C. 1999, *A&A*, 345, 471
 Ryabchikova, T. A., Piskunov, N., Stempels, H. C., Kupka, F., & Weiss, W. W. 1999, *Phys. Scr.*, T83, 162
 Schaller, G., Schaerer, D., Meynet, G. & Maeder, A., 2004, *A&AS* 96, 269
 Shuliak, D., Tsymbal V., Ryabchikova T., Stütz Ch., & Weiss, W.W., 2004, *A&A* 428, 993
 Stauffer, J., Hartmann, L. W., Jones, B. F., & McNamara, B. 1989, *ApJ*, 342, 285
 Stauffer, J., Hartmann, L. W., Prosser, C.F., et. al. 1997, *ApJ*, 479, 776
 Takeda, Y., Zhao, G., Takada-Hidai, M., et al., 2003, *Chin. J. A&A*, 3, 316
 Valenti, J.A., Piskunov, N., & Johns-Krull, C.M. 1998, *ApJ* 498, 851
 Vidal, C.R., Cooper, J., & Smith, E.W. 1973, *ApJS*, 25, 37
 Wolff, S.C. 1983, *The A-stars: Problems and Perspectives*, NASA SP-463

Table 2. Starting and final set of atmospheric parameters. UP – UVES POP number

star	UP	initial set				final set			
		T_{eff}^a	$\log g^a$	$\log g^b$	$v \sin i^c$	T_{eff} [K]	$\log g$ [cgs]	v_{mic} [kms $^{-1}$]	$v \sin i$
HD 73722	04	6550	4.25	4.35	6.8	6480	4.30	1.30	6.7
HD 74044	11	8000	4.20	4.30	32	8130	4.45	2.65	33.7
HD 74275	23	10500	4.42	4.29	62	10200	4.40	1.30	60.5
HD 75029	43	7770	4.20	4.30	24	7800	4.30	2.00	22.0
SHJM 2 ^d	73	5950 ^e		4.40	10.3	6100	4.40	1.15	10.6

^a Obtained from Strömgen photometry^b Obtained using tracks from Schaller 2004^c Taken from Noterdaeme et al. (in prep.)^d Taken from Stauffer et.al (1989)^e Obtained from Johnson UVB photometry**Table 3.** Abundances [$N_{\text{El}}/N_{\text{tot}}$] of members of IC 2391. Solar values according to Grevesse and Sauval (1998)

El	HD 73722			HD 74044			HD 74275			HD 75029			SHJM 2			sun abn
	abn ^a	(err) ^b	[n] ^c	abn	(err)	[n]	abn	(err)	[n]	abn	(err)	[n]	abn	(err)	[n]	
He							-1.08	(-)	[1]							-1.11
C	-3.43	(6)	[4]	-3.47	(-)	[2]							-3.32	(22)	[2]	-3.52
O	-3.10	(-)	[1]	-3.41	(-)	[2]	-3.24	(-)	[2]							-3.21
Na	-5.82	(4)	[4]				-5.03	(24)	[2]				-5.80	(8)	[4]	-5.71
Mg	-4.53	(7)	[5]	-4.45	(5)	[6]	-4.19	(6)	[7]	-4.44	(38)	[5]	-4.41	(9)	[3]	-4.46
Al							-5.21	(-)	[1]				-5.82	(1)	[2]	-5.57
Si	-4.96	(26)	[20]	-4.83	(17)	[6]	-4.52	(24)	[3]	-4.48	(25)	[10]	-4.74	(30)	[19]	-4.49
S	-4.90	(2)	[4]	-4.81	(3)	[3]				-4.92	(5)	[6]	-4.74	(-)	[1]	-4.71
Ca	-5.71	(26)	[29]	-5.64	(9)	[10]	-5.64	(5)	[2]	-6.02	(37)	[10]	-5.46	(7)	[13]	-5.68
Sc	-8.92	(10)	[9]	-8.61	(13)	[3]	-9.18	(-)	[1]	-9.36	(27)	[3]	-8.89	(13)	[6]	-8.87
Ti	-7.14	(7)	[51]	-6.27	(25)	[15]	-6.98	(7)	[6]	-7.17	(21)	[18]	-6.97	(13)	[29]	-7.02
V	-8.24	(10)	[5]										-8.02	(6)	[9]	-8.04
Cr	-6.39	(7)	[37]	-5.75	(11)	[21]	-6.27	(7)	[8]	-6.20	(21)	[24]	-6.23	(10)	[20]	-6.37
Mn	-6.80	(9)	[18]	-6.33	(-)	[1]				-6.44	(12)	[2]	-6.56	(6)	[9]	-6.65
Fe	-4.59	(10)	[298]	-4.19	(12)	[147]	-4.45	(12)	[29]	-4.41	(17)	[96]	-4.46	(9)	[169]	-4.54
Co	-7.31	(3)	[4]										-7.17	(7)	[6]	-7.12
Ni	-5.91	(7)	[50]	-5.34	(6)	[11]				-5.75	(29)	[17]	-5.82	(7)	[32]	-5.79
Cu	-8.20	(13)	[2]	-7.17	(-)	[1]				-7.85	(-)	[1]	-7.76	(-)	[1]	-7.83
Zn	-7.74	(-)	[1]	-7.13	(-)	[1]							-7.55	(-)	[1]	-7.44
Sr	-8.76	(37)	[2]				-9.32	(-)	[1]				-8.77	(36)	[3]	-9.07
Y	-9.82	(3)	[6]	-9.49	(-)	[1]				-9.96	(7)	[2]	-9.74	(9)	[4]	-9.80
Zr	-9.44	(-)	[1]										-9.48	(11)	[2]	-9.44
Ba	-9.53	(19)	[3]	-8.46	(16)	[3]							-9.30	(2)	[2]	-9.91
Ce	-10.48	(-)	[2]	-9.70	(-)	[1]							-10.40	(-)	[2]	-10.46
Nd	-10.40	(9)	[5]										-10.25	(8)	[2]	-10.54
Eu													-11.27	(-)	[1]	-11.53

^a abn element abundance: $[N_{\text{El}}/N_{\text{tot}}] = {}^{10}\log(N_{\text{Element}}/N_{\text{Total}})$ ^b (err) internal errors in units of the last digit^c [n] number of lines used for the final iteration step

Online Material

Table 4. Lines used for abundance determination of HD 74044.

Identity	λ [Å]	logg f									
Cl	4932.049	-1.884	Cr2	5308.408	-1.846	Fe1	5107.447	-3.087	Fe1	5572.842	-0.275
Cl	6014.834	-1.585	Cr2	5310.687	-2.280	Fe1	5107.641	-2.418	Fe1	5576.089	-1.000
O1	6158.176	-0.996	Cr2	5313.563	-1.650	Fe1	5121.639	-0.810	Fe1	5586.756	-0.120
O1	6158.186	-0.409	Cr2	5334.869	-1.562	Fe1	5125.117	-0.140	Fe1	5615.644	0.050
Mg2	4481.126	0.740	Cr2	5407.604	-2.151	Fe1	5133.689	0.140	Fe1	5624.542	-0.755
Mg2	4481.150	-0.560	Cr2	5478.365	-1.908	Fe1	5139.252	-0.741	Fe1	5633.947	-0.270
Mg1	4702.991	-0.666	Cr2	5508.606	-2.110	Fe1	5139.463	-0.509	Fe1	5686.530	-0.446
Mg1	5172.684	-0.402	Cr2	5510.702	-2.452	Fe1	5148.036	-0.629	Fe1	5709.378	-1.028
Mg1	5183.604	-0.180	Cr2	6089.632	-1.265	Fe1	5148.225	-0.274	Fe1	5731.762	-1.300
Mg1	5528.405	-0.620	Mn1	6021.819	0.034	Fe1	5159.058	-0.820	Fe1	5775.081	-1.298
Si1	5675.417	-1.030	Fe1	4438.343	-1.630	Fe1	5162.273	0.020	Fe1	5862.353	-0.058
Si1	5747.667	-0.780	Fe1	4447.717	-1.342	Fe2	5197.577	-2.100	Fe1	5930.180	-0.230
Si1	6145.016	-0.820	Fe1	4466.552	-0.600	Fe1	5202.336	-1.838	Fe1	6020.169	-0.270
Si1	6243.815	-0.770	Fe2	4472.929	-3.430	Fe1	5229.845	-1.127	Fe1	6024.058	-0.120
Si1	6244.466	-0.690	Fe1	4476.019	-0.819	Fe1	5229.880	-0.236	Fe1	6027.051	-1.089
Si1	6254.188	-0.600	Fe1	4476.077	-0.370	Fe2	5234.625	-2.230	Fe1	6056.005	-0.460
S1	6743.531	-0.920	Fe1	4484.220	-0.864	Fe1	5250.646	-2.181	Fe1	6065.482	-1.530
S1	6748.837	-0.600	Fe1	4485.676	-1.020	Fe1	5253.462	-1.573	Fe2	6084.111	-3.780
S1	6757.171	-0.310	Fe2	4491.405	-2.700	Fe2	5254.929	-3.227	Fe2	6113.322	-4.110
Ca1	4425.437	-0.286	Fe1	4494.563	-1.136	Fe1	5273.164	-0.993	Fe1	6127.907	-1.399
Ca2	5019.971	-0.501	Fe2	4508.288	-2.250	Fe1	5273.374	-2.158	Fe2	6147.741	-2.721
Ca1	5581.965	-0.569	Fe2	4515.339	-2.450	Fe1	5281.790	-0.834	Fe2	6149.258	-2.720
Ca1	5588.749	0.313	Fe2	4520.224	-2.600	Fe1	5288.525	-1.508	Fe1	6191.558	-1.417
Ca1	5590.114	-0.596	Fe2	4522.634	-2.030	Fe1	5302.302	-0.720	Fe1	6230.723	-1.281
Ca1	5857.451	0.257	Fe1	4528.614	-0.822	Fe2	5316.615	-1.850	Fe1	6232.641	-1.223
Ca1	6122.217	-0.386	Fe2	4541.524	-2.790	Fe2	5316.784	-2.760	Fe2	6238.392	-2.630
Ca1	6162.173	-0.167	Fe2	4555.893	-2.160	Fe1	5324.179	-0.103	Fe1	6252.555	-1.687
Ca1	6439.075	0.394	Fe2	4576.340	-2.920	Fe2	5325.553	-3.120	Fe1	6265.134	-2.550
Ca1	6717.681	-0.596	Fe2	4583.837	-1.860	Fe1	5341.024	-1.953	Fe1	6336.824	-0.856
Sc2	5031.021	-0.400	Fe1	4602.941	-2.209	Fe1	5353.374	-0.840	Fe2	6369.462	-4.160
Sc2	5239.813	-0.765	Fe1	4607.647	-1.545	Fe2	5362.869	-2.739	Fe2	6383.722	-2.070
Sc2	5526.790	0.024	Fe1	4611.284	-1.017	Fe1	5367.467	0.443	Fe1	6393.601	-1.432
Ti2	4450.482	-1.510	Fe2	4620.521	-3.240	Fe1	5373.709	-0.860	Fe1	6411.649	-0.595
Ti2	4468.507	-0.600	Fe1	4625.045	-1.340	Fe1	5383.369	0.645	Fe2	6416.919	-2.650
Ti2	4518.327	-2.640	Fe1	4632.912	-2.913	Fe1	5389.479	-0.410	Fe1	6419.950	-0.240
Ti2	4529.474	-1.650	Fe2	4635.316	-1.650	Fe1	5391.461	-0.825	Fe1	6421.351	-2.027
Ti2	4552.294	-2.890	Fe1	4643.463	-1.147	Fe1	5393.168	-0.715	Fe1	6430.846	-2.006
Ti1	4552.453	-0.340	Fe1	4654.605	-1.077	Fe1	5400.502	-0.160	Fe2	6446.410	-1.960
Ti2	4563.761	-0.790	Fe1	4678.846	-0.833	Fe1	5405.775	-1.844	Fe1	6677.987	-1.418
Ti2	4571.968	-0.230	Fe1	4707.275	-1.080	Fe1	5410.910	0.398	Ni1	4604.982	-0.250
Ti2	4589.958	-1.620	Fe1	4903.310	-0.926	Fe1	5415.199	0.642	Ni1	4714.408	0.260
Ti2	5010.212	-1.300	Fe1	4920.503	0.068	Fe1	5424.068	0.520	Ni1	4715.757	-0.320
Ti2	5185.913	-1.370	Fe2	4923.927	-1.320	Fe2	5427.826	-1.664	Ni1	4904.407	-0.170
Ti2	5188.680	-1.050	Fe1	4930.315	-1.201	Fe1	5429.505	-1.016	Ni1	5115.389	-0.110
Ti2	5211.536	-1.356	Fe1	4946.388	-1.170	Fe1	5429.697	-1.879	Ni1	5176.559	-0.440
Ti2	5418.751	-2.110	Fe1	4962.572	-1.182	Fe1	5429.827	-0.527	Ni1	5663.975	-0.430
Ti2	5490.690	-2.650	Fe1	4966.089	-0.871	Fe2	5432.967	-3.629	Ni1	5694.977	-0.610
Cr2	4539.595	-2.290	Fe1	4973.102	-0.950	Fe1	5434.524	-2.122	Ni1	5715.066	-0.352
Cr2	4558.650	-0.449	Fe1	4962.572	-1.182	Fe1	5445.042	-0.020	Ni1	6086.276	-0.530
Cr2	4565.740	-1.820	Fe1	4966.089	-0.871	Fe1	5446.917	-1.914	Ni1	6176.807	-0.260
Cr2	4588.199	-0.627	Fe1	4973.102	-0.950	Fe1	5455.441	0.291	Cu1	5105.537	-1.516
Cr2	4634.070	-0.990	Fe1	4988.950	-0.890	Fe1	5455.610	-2.091	Zn1	4722.153	-0.338
Cr1	4646.148	-0.700	Fe2	5004.195	0.497	Fe1	5473.901	-0.760	Y2	5200.406	-0.570
Cr1	4652.152	-1.030	Fe2	5018.440	-1.220	Fe1	5497.516	-2.849	Ba2	4554.029	0.170
Cr1	5204.506	-0.208	Fe1	5044.211	-2.038	Fe2	5529.932	-1.875	Ba2	5853.668	-1.000
Cr2	5237.329	-1.160	Fe1	5049.820	-1.355	Fe1	5554.895	-0.440	Ba2	6141.713	-0.076
Cr2	5249.437	-2.489	Fe2	5061.718	0.217	Fe1	5560.212	-1.190	Ce2	4562.359	0.310
Cr2	5279.876	-2.100	Fe1	5065.014	-0.134	Fe1	5565.704	-0.285			
Cr2	5280.054	-2.011	Fe1	5074.748	-0.200	Fe1	5569.618	-0.486			

Table 5. Selected lines ($[n] < 5$) used for abundance determination of HD 73722, HD 74275, HD 75029 and SHJM 2.

HD 73722			HD 74275			HD 75029			SHJM 2		
Identity	$\lambda[\text{\AA}]$	$\log gf$									
C1	4770.026	-2.439	He1	5875.615	0.409	Sc2	5031.021	-0.400	C1	4932.049	-1.884
C1	4932.049	-1.884	O1	6156.756	-0.899	Sc2	5239.813	-0.765	C1	5380.337	-1.842
C1	5052.167	-1.648	O1	6158.186	-0.409	Sc2	5526.790	0.024	Na1	4497.657	-1.560
C1	5380.337	-1.842	Na1	5889.951	0.117	Mn1	5377.637	-0.109	Na1	5688.205	-0.450
O1	6156.776	-0.694	Na1	5895.924	-0.184	Mn1	6021.819	0.034	Na1	6154.226	-1.560
Na1	5682.633	-0.700	Al2	4663.046	-0.284	Cu1	5105.537	-1.516	Na1	6160.747	-1.260
Na1	5688.205	-0.450	Si2	5978.930	0.004	Y2	5087.416	-0.170	Mg1	4167.271	-1.004
Na1	6154.226	-1.560	Si2	6347.109	0.297	Y2	5200.406	-0.570	Mg1	4571.096	-5.691
Na1	6160.747	-1.260	Si2	6371.371	-0.003				Mg1	5711.088	-1.833
S1	4695.443	-1.920	Ca1	4226.728	0.265				Al1	6696.023	-1.347
S1	4696.252	-2.140	Ca1	4454.779	0.335				Al1	6698.673	-1.647
S1	6052.583	-1.330	Sc2	4246.822	0.242				S1	6052.674	-0.740
S1	6757.171	-0.310	Sr2	4215.519	-0.145				Cu1	5105.537	-1.516
Co1	4792.846	-0.067							Zn1	4722.153	-0.338
Co1	5212.691	-0.110							Sr2	4161.792	-0.502
Co1	5342.695	0.690							Sr2	4215.519	-0.145
Co1	5352.045	0.060							Sr1	4607.327	-0.570
Cu1	5105.537	-1.516							Y2	5087.416	-0.170
Cu1	5218.197	0.476							Y2	5119.112	-1.360
Zn1	4722.153	-0.338							Y2	5402.774	-0.510
Sr2	4161.792	-0.502							Y2	5544.611	-1.090
Sr1	4607.327	-0.570							Zr2	4208.977	-0.460
Zr2	4208.977	-0.460							Zr2	5112.297	-0.590
Ba2	4166.000	-0.420							Ba2	4554.029	0.170
Ba2	5853.668	-1.000							Ba2	5853.668	-1.000
Ba2	6496.897	-0.377							Ce2	4562.359	0.310
Ce2	4562.359	0.310							Ce2	4628.161	0.220
Ce2	4628.161	0.220							Nd2	4706.543	-0.775
									Nd2	5311.453	-0.437
									Eu2	4205.042	0.120